

Study of the $F^{19}(\text{He}^3, d)\text{Ne}^{20}$ Reaction*

R. H. SIEMSEN AND L. L. LEE, JR.
Argonne National Laboratory, Argonne, Illinois

AND

DOUGLAS CLINE
University of Rochester, Rochester, New York
(Received 20 July 1965)

The reaction $F^{19}(\text{He}^3, d)\text{Ne}^{20}$ has been studied at He^3 energies of 9.5 and 10.0 MeV. Angular distributions have been measured for deuteron groups leading to final states in Ne^{20} up to an excitation of 7.43 MeV. The elastic scattering of 9.0-MeV He^3 on F^{19} has also been measured. The reaction data have been analyzed by use of the zero-range distorted-wave Born approximation and spectroscopic information has been extracted. Angular distributions characteristic of a stripping mechanism were observed for the reactions to the ground state ($l_p=0$), 1.63-MeV state ($l_p=2$), 5.80-MeV state ($l_p=1$), 6.72-MeV state ($l_p=0$), and 7.43-MeV state ($l_p=2$). The reactions to the 4.25-, 4.97-, 5.63-, and 7.02-MeV excited states had small cross sections with little angular structure and were probably excited by other reaction mechanisms. The results are in reasonable agreement with the predictions of both the Nilsson model and the extreme $SU(3)$ classification of the shell model that assumes a dominant long-range quadrupole residual interaction.

INTRODUCTION

THE energy-level scheme of the nucleus Ne^{20} can be interpreted in terms of both the collective model¹ and the extreme $SU(3)$ classification of the shell model in which a dominant long-range quadrupole residual interaction is included.^{2,3} A considerable amount of experimental effort, notably by the Chalk River group,⁴ has been expended in determining the spins, parities, and electromagnetic properties of the levels in Ne^{20} . Three positive-parity and two negative-parity rotational bands have so far been identified.¹

Spectroscopic information extracted from direct-reaction measurements is another good test of the applicability of different models to Ne^{20} . Studies of the $F^{19}(d, n)\text{Ne}^{20}$ reaction^{5,6} yielded spectroscopic information for the transitions to the ground state and the levels at 1.63- and 6.75-MeV excitation. However, a measurement of the angular distributions of the transitions to the negative-parity states in Ne^{20} from the $F^{19}(d, n)\text{Ne}^{20}$ reaction at 3 MeV did not yield conclusive evidence as to the stripping contribution to the reaction amplitude because of the low bombarding energy.⁶

The (He^3, d) reaction, which is the analog of the (d, n) reaction, has obvious experimental advantages, and recent work^{7,8} indicates that this reaction can give

reliable quantitative spectroscopic information when treated as a direct stripping reaction. The ground-state and first-excited-state transitions from the $F^{19}(\text{He}^3, d)\text{Ne}^{20}$ reaction have been studied previously by Jahr⁹ at a bombarding energy of 13 MeV. The present measurements of the $F^{19}(\text{He}^3, d)\text{Ne}^{20}$ reaction were undertaken to gain more detailed spectroscopic information than was obtained from the analog reaction. Angular distributions of 10 deuteron groups have been measured and the reaction data have been analyzed by use of the zero-range distorted-wave (DW) code JULIE.¹⁰ The elastic scattering of He^3 by F^{19} has also been measured at 9.00 MeV. Optical-model parameters for use in the distorted-wave calculation have been obtained from an analysis of these elastic-scattering data.

EXPERIMENT

Angular distributions of the $F^{19}(\text{He}^3, d)\text{Ne}^{20}$ reaction have been measured with the University of Rochester cyclotron and with the Argonne tandem Van de Graaff at bombarding energies of 9.5 and 10.0 MeV, respectively. The measurements at Argonne were done in an 18-in. scattering chamber, designed by T. H. Braid and J. T. Heinrich, and the particles were identified with a $dE \times E$ solid-state counter telescope and a pulse-multiplier circuit similar to that described by Stokes.¹¹ The separation of the different particle groups was continuously monitored with a two-dimensional multi-channel analyzer. At far forward angles, a gold foil in front of the detector telescope was used to absorb scattered He^3 particles. Angular distributions of the $F^{19}(\text{He}^3, d)\text{Ne}^{20}$ reaction were measured with improved

*Work performed under the auspices of the U. S. Atomic Energy Commission.

¹A. E. Litherland, J. A. Kuehner, H. E. Gove, M. A. Clark, and E. Almqvist, Phys. Rev. Letters **7**, 98 (1961).

²J. P. Elliott, Proc. Roy. Soc. (London) **A245**, 128 and 562 (1958); J. P. Elliott and M. Harvey, *ibid.* **A272**, 557 (1963).

³M. Harvey (private communication).

⁴H. C. Evans, M. A. Eswaran, H. E. Gove, A. E. Litherland, and C. Broude, Can. J. Phys. **43**, 82 (1965).

⁵J. M. Calvert, A. A. Jaffe, and E. E. Maslin, Proc. Phys. Soc. (London) **A68**, 1017 (1955).

⁶R. H. Siemssen, R. Felst, M. Cosack, and J. L. Weil, Nucl. Phys. **52**, 273 (1964).

⁷A. G. Blair, Argonne National Laboratory Report ANL-6878, p. 115 (unpublished).

⁸R. H. Bassel, R. M. Drisko, and G. R. Satchler, in Oak Ridge

National Laboratory Report ORNL-3800, 1965, p. 54 (unpublished).

⁹R. Jahr, Phys. Rev. **129**, 320 (1963).

¹⁰R. H. Bassel, R. M. Drisko, and G. R. Satchler, Oak Ridge National Laboratory Report ORNL-3240, 1962 (unpublished).

¹¹R. H. Stokes, Rev. Sci. Instr. **31**, 768 (1960).

energy resolution by use of a broad-range magnetic spectrograph in conjunction with the 27-in. variable-energy cyclotron at the University of Rochester. Deuteron groups leading to states with an excitation of up to 7.5 MeV in Ne^{20} were observed with an energy resolution width of 60 keV. All measurements were performed with thin CaF_2 targets evaporated onto thin carbon backings.

The elastic scattering was measured at the Université Laval 6-MeV Van de Graaff by scattering the 9-MeV $(\text{He}^3)^{++}$ beam off a $35\text{-}\mu\text{g}\text{-cm}^{-2}$ target of CaF_2 deposited on a $30\text{-}\mu\text{g}\text{-cm}^{-2}$ carbon backing. The scattered He^3 were detected by a position-indicating surface-barrier detector in the focal plane of the magnetic spectrograph. The elastic scattering from C^{12} , O^{16} , F^{19} , and Ca^{40} was clearly resolved down to angles of 15° . The absolute cross section for the elastic scattering was obtained by reference to the elastic scattering from Ca^{40} which obeys the Rutherford formula out to 25° . The target composition was checked by studying the elastic scattering of a 4.5-MeV He^3 beam, since at this energy the elastic scattering by both Ca^{40} and F^{19} obeys the Rutherford formula out to 30° . The target was found to contain two F atoms to one Ca atom to within an accuracy of 4%. Absolute cross sections for the reaction data were similarly obtained by comparing the reaction yields of He^3 elastically scattered from Ca at 5 MeV and at an angle of 60° .

EXPERIMENTAL RESULTS

Deuteron spectra from the reaction $F^{19}(\text{He}^3, d)\text{Ne}^{20}$ obtained with the counter telescope and with the broad-range magnetic spectrograph are shown in Fig. 1. Only the region from ~ 5.5 - to ~ 8.0 -MeV excitation is shown for the magnet results. The level scheme for Ne^{20} is presented in Fig. 2; the spin and parity assignments are taken from the work of Kuehner and Pearson¹² and the division into rotational bands is that suggested by the Chalk River group.¹ The angular distribution for the elastic scattering of He^3 by F^{19} , plotted as a ratio to the Rutherford cross section, is shown in Fig. 3. The statistical errors are equal to or less than the point sizes in Fig. 3. The error in the absolute cross section is estimated to be $\pm 5\%$.

The $F^{19}(\text{He}^3, d)\text{Ne}^{20}$ reaction data taken with the magnetic spectrograph and with the $dE \times E$ telescope were in good agreement for the deuteron groups resolved in both experiments. Deuteron groups leading to all the known levels¹² in Ne^{20} up to an excitation of 7.43 MeV were observed with the magnetic spectrograph, although the groups populating the 7.17- and 7.20-MeV levels were unresolved. No other deuteron groups are observed. The deuteron groups leading to the 7.02-, 7.17-, and 7.20-MeV levels were also unresolved in the counter-telescope data. The results for the $F^{19}(\text{He}^3, d)\text{Ne}^{20}$ reaction are presented in Figs. 4 and 5. The data shown for

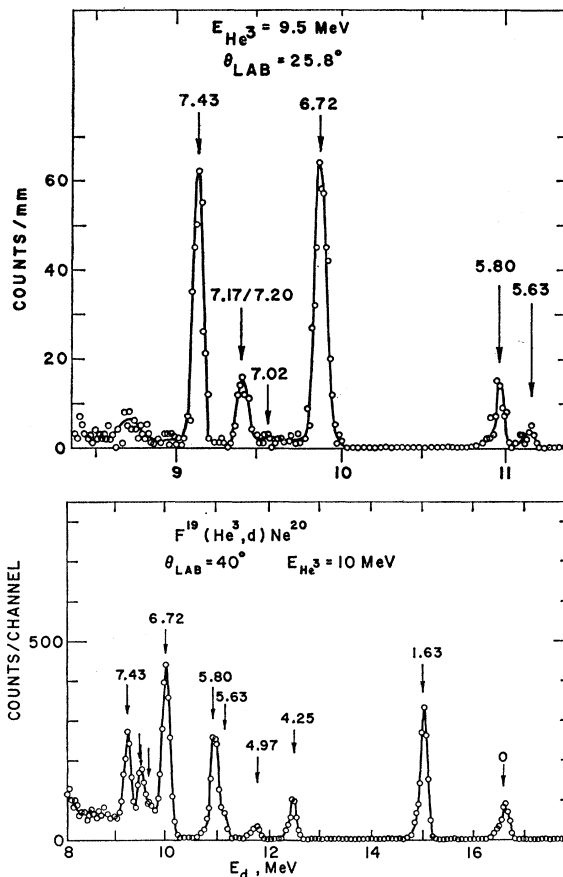


FIG. 1. Deuteron spectra from the reaction $F^{19}(\text{He}^3, d)\text{Ne}^{20}$ observed with a counter telescope (lower portion) at Argonne and with a broad-range spectrograph (upper portion) at Rochester. The spectrograph data are shown only for the region from 5.5- to 8.0-MeV excitation in Ne^{20} . The excitation energies of the various peaks, as given by Ref. 12, are shown on the figure.

the transitions to the ground state and first three excited states include only the counter-telescope results because their statistical accuracy was much superior to that of the spectrograph data. The combined data from both experiments are presented for the transitions to the more closely spaced higher excited states.

The absolute normalization for the magnetic-spectrograph data was obtained by comparison with the counter-telescope data for the deuteron group leading to the 1.63-MeV state. The error in the absolute cross section for the reaction data is estimated to be $\pm 15\%$. The angle setting was accurate to 0.3° . The angular-distribution data for both the ground state and first excited state are in good agreement both in shape and magnitude with the measurements of Jahr⁹ at 13-MeV incident energy. As may be seen from the figures, the transitions to the ground state and excited states of Ne^{20} at 1.63-, 5.80-, 6.72-, and 7.43-MeV excitation have angular distributions characteristic of a stripping reaction. For these cases, theoretical angular distributions calculated with the distorted-wave Born

¹² J. A. Kuehner and J. D. Pearson, Can. J. Phys. 42, 477 (1964).

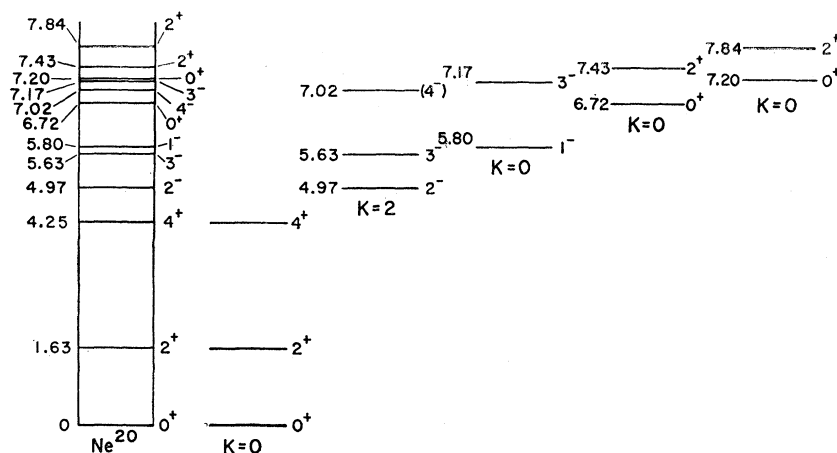


FIG. 2. Energy-level diagram for Ne^{20} with the energies, spins, and parities as given by Ref. 1. The entire level structure is shown in the left column. The other columns represent the division into rotational bands as suggested by Ref. 1 with the appropriate K quantum numbers indicated.

approximation (DWBA) method are shown for comparison. The angular distribution of the transition to the 4.25-MeV 4^+ level is nearly symmetric about 90° while the weakly excited levels at 4.97, 5.63, and 7.02 MeV show little angular structure. A comparison of the cross section for the 7.20-MeV unresolved doublet with that for the 0^+ 6.72-MeV level shows that the $l=0$ stripping reaction to the 7.20-MeV 0^+ member of the doublet must be weak. An upper limit for the cross section to the 7.20-MeV doublet at 0° has been determined to be 2 mb/sr from the counter-telescope data.

DW AND OPTICAL-MODEL ANALYSIS OF THE DATA

The optical-model parameters for the incoming channel in the DW analysis of the $F^{19}(He^3, d)Ne^{20}$ reaction were obtained from an analysis of the He^3

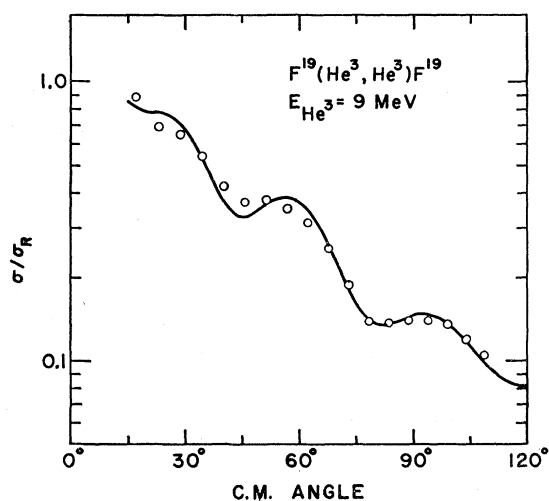


FIG. 3. Angular distribution of 9.0-MeV He^3 elastically scattered from F^{19} , plotted as the ratio to Rutherford scattering. The statistical errors are smaller than the point sizes; the uncertainty in the absolute cross section is estimated to be about 5%. The solid line is an optical-model fit for the parameters given in Table I.

elastic-scattering data presented here by use of the optical-model least-squares search codes HUNTER¹³ and JIB3.¹⁴ A Woods-Saxon form factor was chosen both for the real and imaginary potentials, the imaginary potential possessing a radius 70% greater than that for the real potential. Bassel¹⁵ has found these radial parameters to best explain the systematics of He^3 scattering data. Aside from the well-known Vr^n ambiguities, many sets of optical-model parameters would equally well explain the elastic-scattering data.¹⁶ However, previous studies¹⁷⁻¹⁹ of both the elastic scattering of He^3 and the (He^3, α) reaction on the target nuclei O^{16} , K^{39} , and Ca^{40} showed that only one of these types of potentials would also explain the (He^3, α) reaction data, namely a potential with a real well depth around 160 MeV. The least-squares optical-model parameters, given in Table I, differed only slightly from the parameters found to best explain the elastic scattering of He^3 by O^{16} , K^{39} , and Ca^{40} at the same incident energy.¹⁷⁻¹⁹ In Fig. 3, the elastic-scattering cross sections calculated by use of the optical-model parameters given in Table I are compared with the data.

Since no elastic-scattering data are available for 15-MeV deuterons scattered by Ne^{20} , optical-model parameters of the exit $d+Ne^{20}$ channel were taken similar to those found to best explain the elastic scattering of deuterons²⁰ by Ca^{40} ; these parameters are also given in Table I. This potential has a Woods-Saxon shape for the real potential well and a surface-derivative form factor for the imaginary potential.

¹³ R. M. Drisko (private communication).

¹⁴ F. Perey (unpublished notes).

¹⁵ R. H. Bassel (private communication).

¹⁶ R. M. Drisko, G. R. Satchler, and R. H. Bassel, Phys. Letters 5, 347 (1963).

¹⁷ W. P. Alford, L. M. Blau, and D. Cline, Nucl. Phys. 61, 368 (1965).

¹⁸ D. Cline, W. P. Alford, and L. M. Blau, Nucl. Phys. (to be published).

¹⁹ L. M. Blau, W. P. Alford, D. Cline, and H. E. Gove, Nucl. Phys. (to be published).

²⁰ R. H. Bassel, R. M. Drisko, G. R. Satchler, L. L. Lee, Jr., J. P. Schiffer, and B. Zeidman, Phys. Rev. 136, B960 (1964).

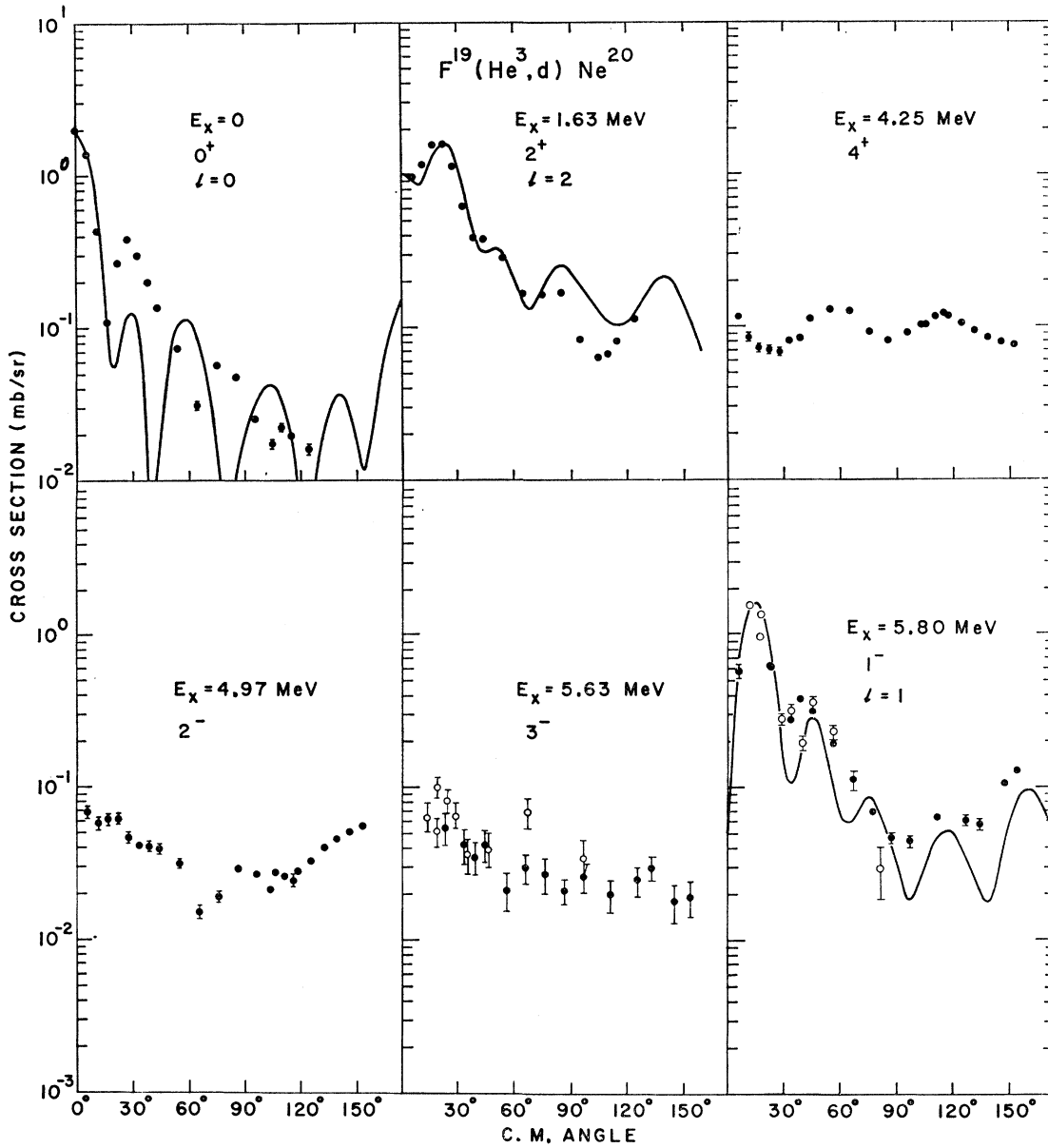


FIG. 4. Deuteron angular distributions from the reaction $F^{19}(\text{He}^3, d)\text{Ne}^{20}$ to the final states indicated. The solid points represent data taken with the counter telescope, the open circles are results from the magnetic-spectrograph runs. Statistical errors are shown when larger than the point sizes; absolute cross sections are estimated to be accurate to 15%. The solid lines represent normalized DWBA fits for those transitions that are believed to proceed by a stripping mechanism. The parameters for these curves are listed in Table I and the spectroscopic factors obtained from the normalization are listed in Table II. The l values and known spins and parities of the states are indicated in the figure.

TABLE I. Optical-model parameters used in distorted-wave analysis of the $F^{19}(\text{He}^3, d)\text{Ne}^{20}$ reaction. The potential used was $U = V_e - [V/(1+e^x)] - i[W/(1+e^x) + 4W'e^{x'}/(1+e^{x'})^2]$, where $x = (r - r_0 A^{1/3})/a$ and $x' = (r - r_w A^{1/3})/a_w$.

	V (MeV)	W (MeV)	r_0 (F)	a (F)	r (F)	r_w (F)	a_w (F)	W' (MeV)
Incoming $\text{He}^3 + F^{19}$ channel	166.2	18.1	1.05	0.829	1.40	1.81	0.592	0
Outgoing $d + \text{Ne}^{20}$ channel	100.0	0	1.00	0.900	1.40	1.85	0.500	10.0

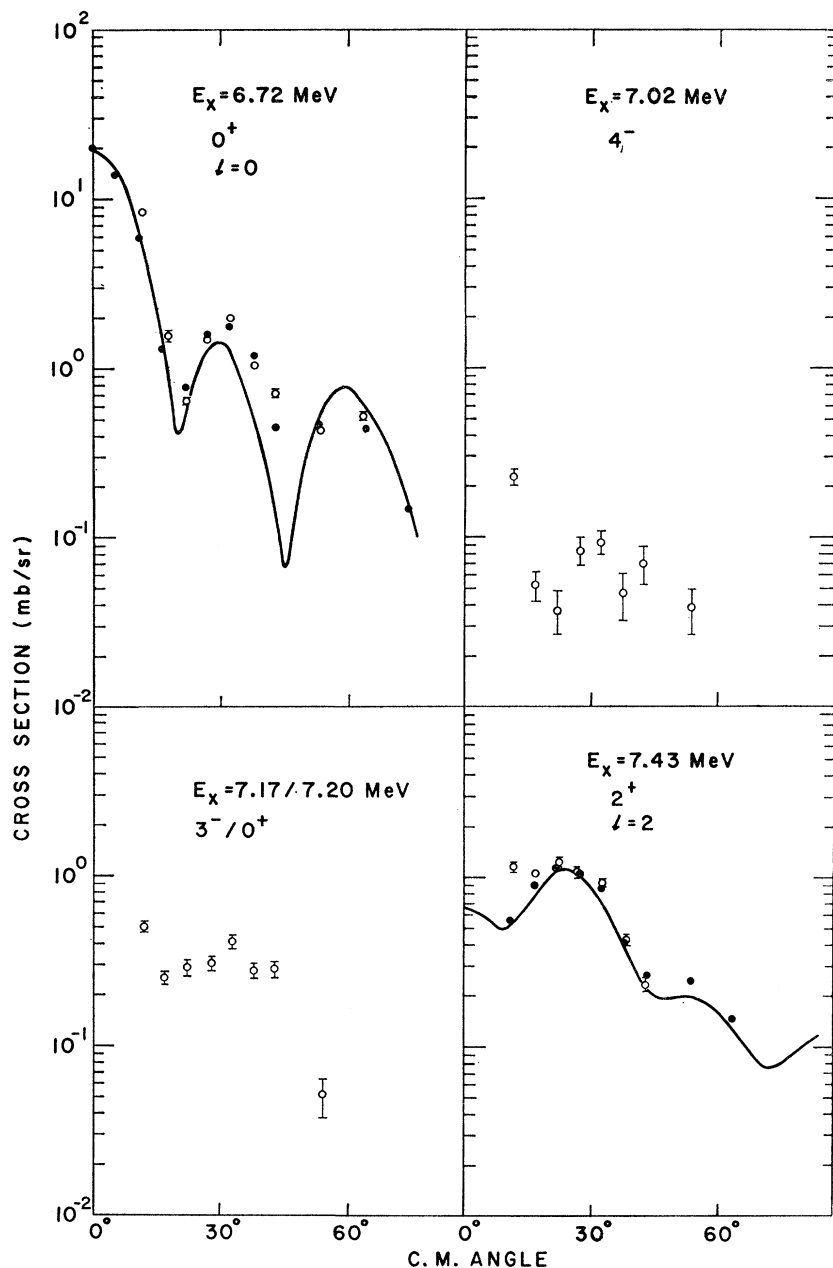


FIG. 5. Deuteron angular distributions from the reaction $F^{19}(\text{He}^3, d)\text{Ne}^{20}$ to the final states indicated. For these states, data were obtained only in the angular range $0^\circ \leq \theta \leq 75^\circ$. The solid points represent data taken with the counter telescope, the open circles are results from the magnetic-spectrograph runs. Statistical errors are shown when larger than the point sizes; absolute cross sections are estimated to be accurate to 15%. The solid lines represent normalized DWBA fits for those transitions that are believed to proceed by a stripping mechanism. The parameters for these curves are listed in Table I and the spectroscopic factors obtained from the normalization are listed in Table II. The l values and known spins and parities of the states are indicated on the figure.

The optical-model parameters from Table I were used to compare the data with the zero-range DW code JULIE.¹⁰ The bound-state wave function was computed for a proton in a Woods-Saxon potential with a radius parameter 1.2 F and diffuseness 0.65 F. The well depth was chosen to place the appropriate level at the separation energy. Except for the unnatural-parity 2^- state at 4.97-MeV excitation, the possible orbital angular momenta of the transferred protons are uniquely determined by the spins and the parities of the initial and final states in the $F^{19}(\text{He}^3, d)\text{Ne}^{20}$ reaction.

The predictions of the zero-range DW calculations for the strongest transitions are compared with the

data in Figs. 4 and 5. To obtain reasonable agreement between the shape of the calculated and experimental angular distributions, it was necessary to suppress the contributions to the reaction from the interior of the nucleus by applying a cutoff radius. The data were best explained with a cutoff radius of 3.9 F. Although this cutoff radius is comparatively large for as light a nucleus as F^{19} , it is similar to the cutoff radius found to give the best agreement in previous investigations in which the angular distributions from the (He^3, α) reaction were fitted by use of similar optical-model parameters.¹⁷⁻¹⁹ Although the agreement between the calculated and experimental angular distributions is

reasonable for the low- Q transitions, there is notably poorer agreement for the ground-state transition.

SPECTROSCOPIC FACTORS

The relation for the absolute cross section can be written in the form

$$\frac{d\sigma}{d\Omega}(\theta) = [(2J_f + 1)/(2J_i + 1)]N \sum S(l_i)\sigma_{l_i}(\theta),$$

where $\sigma_{l_i}(\theta)$ is the reduced cross section evaluated by the DWBA program for the stripping of a proton into an orbit (l, j) , $S(l, j)$ is the spectroscopic factor which contains the nuclear-structure information, the quantities J_i and J_f are the initial and final spins, and the factor N is a term that includes the overlap factor for formation of a He^3 from $d+p$ as well as the strength of the interaction causing the transition. A recent calculation⁸ gives a value of 4.4 for the normalizing factor N . This agrees well with the value found empirically from a zero-range DW analysis of reactions for which the spectroscopic factor was presumably well known.⁷

Spectroscopic factors extracted from the data are listed in Table II. In the following discussion the levels have been separated for clarity into groups which, on a simplified deformed-rotor model, may be considered to be rotational bands.¹ Upper limits have been quoted for the spectroscopic factors for the weak transitions. These upper limits are especially high for those transitions that involve a large angular-momentum transfer and are probably meaningless in these cases. However, the very small spectroscopic factors for the $l_p=1$ stripping to the 4.97-MeV 2^- level and for the $l_p=0$ stripping to the 7.20-MeV 0^+ level are suggestive of some strong selection rule inhibiting these transitions. Except for the ground-state transition, the spectroscopic factors extracted from the data are found to be very little affected by the particular choice of the optical potentials or cutoff radius, the variations being $\lesssim 30\%$. However, the $l_p=0$ ground-state transition was found to be rather sensitive to the optical-model parameters, and the spectroscopic factors differed by a factor of two. The spectroscopic factors obtained from our measurement may be compared with those from the $F^{19}(d, n)\text{Ne}^{20}$ reaction^{6,7} (Table III). Except for the ground-state transition, the spectroscopic factors agree remarkably well. It is interesting to note that the (d, n) spectroscopic factors had been obtained with plane-wave theory by the method outlined by Macfarlane and French.²¹

DISCUSSION

All the observed levels of Ne^{20} up to an excitation of 7.5 MeV have been successfully explained as being composed of five rotational bands¹ which have about

TABLE II. Experimental and theoretical spectroscopic factors for the $F^{19}(\text{He}^3, d)\text{Ne}^{20}$ reaction. The spectroscopic factors predicted by the Nilsson model have been calculated for a deformation $\eta = +4$. It was assumed that the $K=2^-$ band and the $K=0^+$ band at 7.20 MeV are formed by core excitation. The spectroscopic factors predicted by the $SU(3)$ model have been obtained from Ref. 3.

Excitation energy (MeV)	J	L	S_{exp}	Nilsson model	$SU(3)$ model
0.000	0^+	0	0.31	0.41	0.43
1.632	2^+	2	0.63	0.32	0.24
4.248	4^+	4	≤ 0.21	0.0	0.0
$K=2^-$ $(\lambda, \mu) = (8, 2)$					
4.969	2^-	1	≤ 0.001	0.0	0.0
		3	≤ 0.06	0.0	0.0
5.631	3^-	3	≤ 0.042	0.0	0.0
7.02	4^-	3	≤ 0.026	0.0	0.0
$K=0^-$ $(\lambda, \mu) = (9, 0)$					
5.80	1^-	1	0.051	0.08	0.031
7.17	3^-	3	≤ 0.092	0.11	0.014
$K=0^+$ $(\lambda, \mu) = (4, 2)$					
6.72	0^+	0	0.47	0.22	0.17
7.43	2^+	2	0.16	0.15	0.007
$K=0^+$ $(\lambda, \mu) = (0, 4)$ (2, 0)					
7.20	0^+	0	≤ 0.027	0.0	0.0

the same moment of inertia \mathcal{I} ($\hbar^2/2\mathcal{I} \approx 150$ keV). The assumption of rotational bands in Ne^{20} is supported by the recent lifetime measurements by Evans *et al.*,⁴ who have found strongly enhanced $E2$ transitions from the 4.25- and 1.63-MeV states. They also observed that the $E1$ transitions from the 4.97- and 5.63-MeV states are strongly inhibited. This inhibition is greater than one expects from isobaric-spin selection rules and suggests that the ΔK selection rule also applies in agreement with the decomposition of Ne^{20} into rotational bands as suggested by Ref. 1. From the large positive quadrupole moments of the nuclei in the neighborhood of Ne^{20} , it further can be implied that the nuclei in this mass region have a prolate (positive) deformation. The Nilsson single-particle model,²² taken in a spheroidally

TABLE III. Comparison of the spectroscopic factors from the $F^{19}(d, n)\text{Ne}^{20}$ (Refs. 6, 7) and $F^{19}(\text{He}^3, d)\text{Ne}^{20}$ reactions.

Excitation energy in Ne^{20} (MeV)	J	$S_{d, n}$	$S_{\text{He}^3, d}$
0	0^+	0.62	0.34
1.63	2^+	0.70	0.62
6.75	0^+	0.38	0.44

²¹ M. H. Macfarlane and J. B. French, Rev. Mod. Phys. **32**, 567 (1960).

²² S. G. Nilsson, Kgl. Danske Videnskab. Selskab, Mat.-Fys. Medd. **29**, No. 16j (1955).

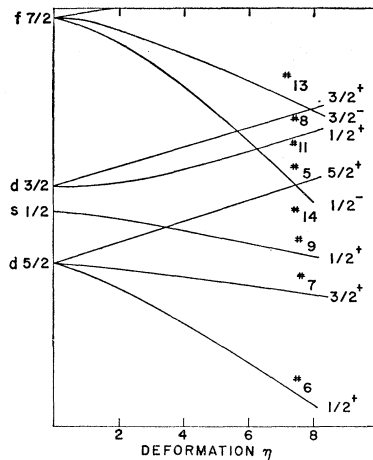


FIG. 6. Energy levels in a spheroidal potential well, computed after the method of Nilsson. The relative energies are depicted as a function of deformation η for the parameters used by Bishop (Ref. 26). The numbers assigned to the levels are the orbit numbers used by Nilsson.

deformed oscillator potential well, explains many of the properties of the nearby odd- A nuclei F^{19} , Ne^{21} , Mg^{25} , and Al^{25} . The best over-all agreement for all these nuclei is found with a deformation parameter η of about $+4$.²³⁻²⁵ The moments of inertia for the rotational bands in these nuclei have about the same value as is found in Ne^{20} .

The success of the Nilsson model in explaining the properties of the nearby odd- A nuclei suggests applying this model to Ne^{20} . For a calculation of spectroscopic factors for comparison with the experimental results, the intrinsic structure for each rotational band has to be known. The single-particle energy levels in a spheroidal potential well are shown in Fig. 6. The numbers assigned to the levels are the orbit numbers used by Nilsson.²² This diagram was obtained from a calculation with Nilsson's potential well, modified by addition of a term μl^2 with $\mu=0.167$. As shown by Bishop,²⁶ the properties of the nearby odd- A nuclei are best explained with this additional term, and we have therefore adopted the parameters suggested by Bishop for the following discussion.

In Ne^{20} , three positive-parity $K=0$ bands are suggested¹ for excitation energies below 7.5 MeV. For a positive deformation, the ground state of Ne^{20} is formed by placing all four particles outside the closed O^{16} shell into the Nilsson orbit 6. If the F^{19} ground state can be assumed to have one proton hole in orbit 6, the 0^+ and 2^+ members of the ground-state rotational band then should be strongly populated²¹ by a stripping reaction—in agreement with the experimental observation. A second $K=0^+$ band that would be strongly populated in the stripping reaction would be the one associated with placing three particles in orbit 6 and the fourth in orbit 9. This presumably is the $K=0^+$ rotational band based on the 6.72-MeV level, for which stripping

transitions have been found both to the 0^+ level at 6.72-MeV excitation and the 2^+ level at 7.40 MeV. The third experimentally observed $K=0^+$ band, which is not strongly excited by the stripping reaction, is probably a two-particle excitation such as two particles in orbit 6 and two in orbit 7. Indeed, if one sums the single-particle energies in the Nilsson model by use of the modified parameters suggested by Bishop²⁶ and a deformation $\eta=+4$, the $(6)^3(9)$ 0^+ state falls at an excitation of 6.5 MeV and the $(6)^2(7)^2$ 0^+ state is at 7.8-MeV excitation. These values are remarkably close to the values of 6.72 and 7.20 MeV suggested by the results of our experiment.

The negative-parity bands can be formed either by lifting a particle from the second to the third oscillator shell or by lifting a particle up out of the filled first harmonic-oscillator shell into the second. The first type of state would be observed in the stripping reaction whereas the second would be forbidden. Experimentally, two negative-parity bands are suggested,¹ a $K=2^-$ for which we observe no stripping and a $K=0^-$ which appears to be appreciably excited in the stripping reaction. The simple Nilsson model predicts many negative-parity bands and does not indicate which is the lowest. As discussed later, the $SU(3)$ model (which is directly related to the Nilsson model) does correctly predict the negative-parity bands. It explains the $K=2^-$ band as being based only on excitations from the $1p$ shell whereas the $K=0^-$ band includes excitations into the $1f_{7/2}$ shell. Thus, by analogy with the $SU(3)$ model, in the Nilsson model the observed $K=0^-$ band can be assumed to be formed by lifting a particle into the lowest of the third harmonic-oscillator levels (Nilsson orbit 14), whereas the $K=2^-$ band can then be assumed to be a $1p$ -shell excitation.

Alternatively, it has been suggested¹ that the negative-parity bands might be explained as rotations of a Ne^{20} nucleus which is undergoing surface octupole vibrations. This interpretation has been supported by recent observations of strong inelastic alpha-particle scattering to the 3^- states at 5.63- and 7.17-MeV excitation.²⁷ Our observation of stripping to the 1^- state at 5.80-MeV excitation is contrary to this explanation of the negative-parity bands, but may not be significant because of the low spectroscopic factor observed.

As shown by Satchler,²⁸ spectroscopic factors predicted by the Nilsson model can be calculated by use of the expression

$$S_{i,j} = g^2 (2I_i + 1/2I_f + 1) (I_i, K_i, j, K_f - K_i | I_f K_f)^2 \times C_{n l_j} (|\Omega|)^2 \delta(|\Omega|, |K_f \pm K_i|)^2 \langle f | i \rangle^2,$$

where I_i and I_f are the spins of the initial and final states, respectively, and K_i and K_f their K quantum numbers; I is the total angular momentum of the

²³ E. B. Paul, *Phil. Mag.* **2**, 311 (1957).

²⁴ A. E. Litherland, H. McManus, E. B. Paul, D. A. Bromley, and H. E. Gove, *Can. J. Phys.* **36**, 378 (1958).

²⁵ K. H. Bhatt, *Nucl. Phys.* **39**, 375 (1963).

²⁶ G. R. Bishop, *Nucl. Phys.* **14**, 376 (1959).

²⁷ A. Springer and B. G. Harvey, *Phys. Rev. Letters* **14**, 316 (1965).

²⁸ G. R. Satchler, *Ann. Phys. (N. Y.)* **3**, 275 (1958).

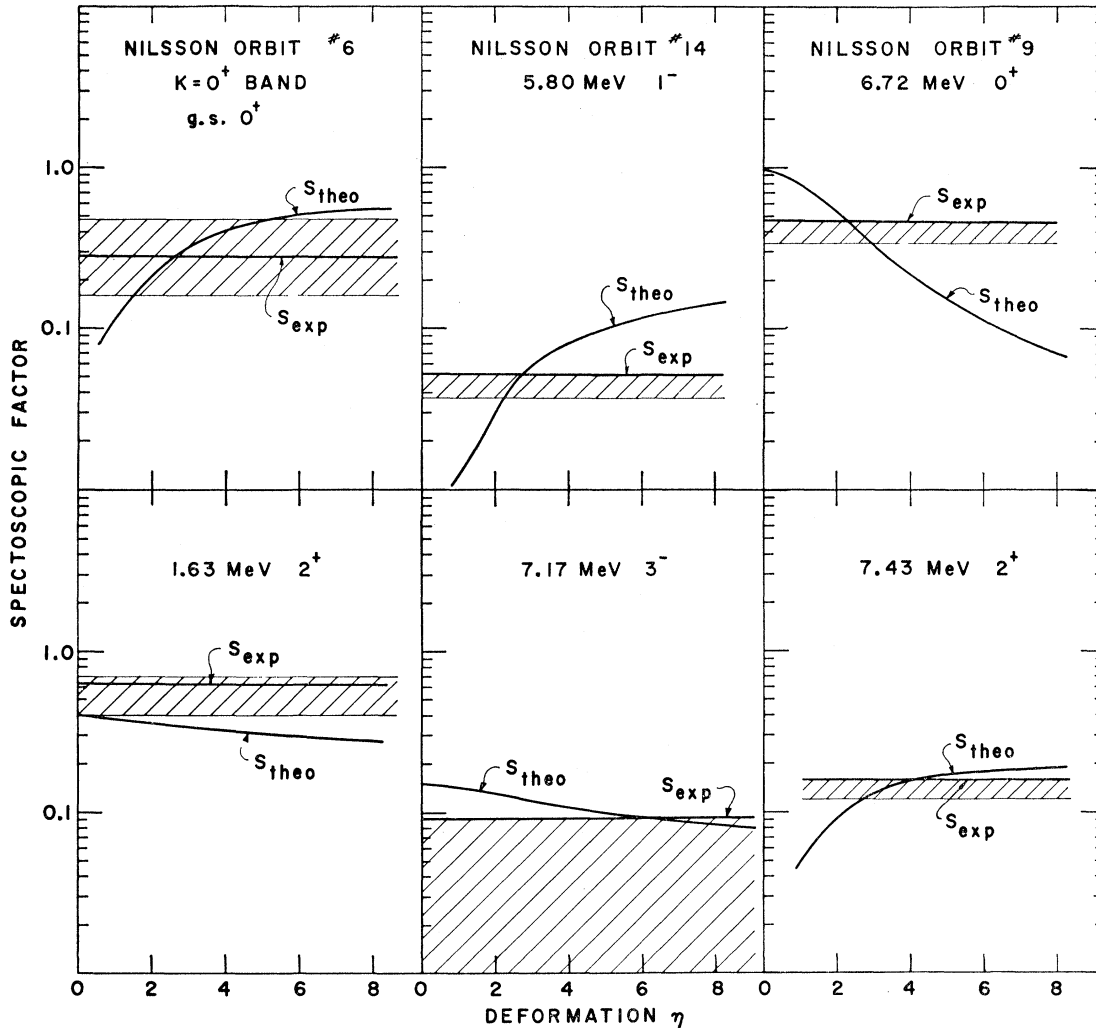


FIG. 7. Spectroscopic factors S . The values determined in the present experiment are compared with predictions based on the Nilsson model as discussed in the text. The measured spectroscopic factors are depicted as a horizontal line and the theoretical predictions are shown as functions of the deformation parameter η . The uncertainties (shaded regions) in the measured spectroscopic factors are due to uncertainties in parameters and to the use of cutoff radii as discussed in the text. The 15% experimental uncertainty in the absolute cross section is not included in this estimate. (g.s. = ground state.)

captured particle; $\langle f|i \rangle$ is the core overlap, which is normally taken to be 1 if the initial and final states are in the same vibrational state; the C_{n_i} are the expansion coefficients of the Nilsson wave function; $g = \sqrt{2}$ in certain cases when either K_i or K_f is zero. In the present study $g = \sqrt{2}$ for the ground-state band. For the other $K=0$ rotational bands in Ne^{20} the rotational factor of $\sqrt{2}$ is canceled by a factor $\frac{1}{2}\sqrt{2}$ which stems from the fact that in constructing intrinsic wave functions with $T = T_z = 0$, neutron and proton excitations must be treated on the same footing.

Spectroscopic factors have been calculated from the above expression with the assumption that the ground-state and the 6.73-MeV $K=0$ bands are formed by capture of a proton into Nilsson orbits 6 and 9, respectively, and the negative-parity $K=0$ band based on the

5.80-MeV level is formed by capture of the proton into orbit 14. We take $g = \sqrt{2}$ for the ground-state rotational band and 1 for all the other bands.²⁹ In Fig. 7 the spectroscopic factors calculated for different deformations η are shown together with the measured spectroscopic factors (horizontal lines); the estimated uncertainties (indicated by the shaded regions) in the experimental spectroscopic factors arise from the ambiguities in the optical potentials and in the cutoff radii. As is seen from Fig. 7, the measured and the calculated spectroscopic factors are of the same order of magnitude although the calculated value for the 1.63-MeV level is only about half the experimental value. Although the deformation parameters η derived

²⁹ In Ref. 6 the theoretical spectroscopic factor for the 6.72-MeV level had been calculated with $g = \sqrt{2}$.

from the comparison of the spectroscopic factors differ appreciably from one state to the other, they do cluster around the expected value of $+4$. As may be seen from Table II, the upper limits placed on the spectroscopic factors for stripping to the $K=2^-$ band are remarkably low, particularly for $l=1$ stripping to the 4.97-MeV 2^- level.

The shell-model approach to the description of Ne^{20} can also be applied within the $SU(3)$ classification scheme after the manner of Elliott.² The simplifying assumptions made in an extreme version of this model are that a long-range quadrupole-quadrupole force dominates the residual interaction and that exchange forces are such that they favor states of maximum orbital symmetry. These are certainly extreme assumptions since it is known that the short-range pairing force is important in nuclei and almost certainly mixes the different $SU(3)$ symmetries significantly. Harvey³ has used this model to calculate the spectroscopic factors for the $\text{F}^{19}(\text{He}^3, d)\text{Ne}^{20}$ reaction. The structure of the ground state of F^{19} was assumed to have the $SU(3)$ classification² $(\lambda, \mu) = (6, 0)$, with $L=0$, $S=\frac{1}{2}$ and $J=\frac{1}{2}$. Making the (λ, μ) assignments listed in Table II for the levels in Ne^{20} led to the spectroscopic factors given. The agreement between experiment and the prediction from the $SU(3)$ model is about as close as that with the Nilsson model. The close agreement between the calculated spectroscopic factors from the Nilsson model and the $SU(3)$ model is reasonable, since in the extreme these models are in essence the same. The agreement of either model with experiment is probably as good as one could expect in view of the very simple assumptions made.

CONCLUSION

The differential cross sections observed in the present experiment for the reaction $\text{F}^{19}(\text{He}^3, d)\text{Ne}^{20}$ are in good agreement with the expectations from describing the level structure of Ne^{20} in terms of rotational bands. The present results are completely consistent with the decomposition into K bands as suggested by the Chalk River group (see Ref. 1.) As discussed in the previous section, detailed comparisons of our measured spectroscopic factors with theoretical predictions require comparison with calculations based on approximate nuclear models. We have compared our results with predictions based on both the Nilsson model and the $SU(3)$ classification of the shell model. These models yield predictions which are quite similar and are in quite good general agreement with our measurements. In view of the crude nature of the models and the difficulties in extracting meaningful spectroscopic factors, it is perhaps quite remarkable that the quantitative comparison of our results with the theoretical predictions comes as close as it does.

ACKNOWLEDGMENTS

The authors are particularly indebted to Dr. Malcolm Harvey for communicating his results and for permission to quote them prior to publication. We are also indebted to Dr. H. E. Gove and Dr. W. P. Alford for help in the experimental work, J. G. McShane for help with the data reduction, and Dr. M. H. Macfarlane for several stimulating discussions. We should also like to thank the Université Laval for the use of their facilities and Dr. C. St. Pierre for his help in the work at Laval.